nature cell biology

Distinct signalling pathways regulate sprouting angiogenesis from the dorsal aorta and the axial vein

David M. Wiley[1], Jun-Dae Kim[2], Jijun Hao[3], Charles C. Hong[3,4], Victoria L. Bautch[1,5,8] and Suk-Won Jin[5,6,7,8]

Angiogenesis, the formation of new blood vessels from pre-existing vessels, is critical to most physiological processes and many pathological conditions. During zebrafish development, angiogenesis expands the axial vessels into a complex vascular network that is necessary for efficient oxygen delivery. Although the dorsal aorta and the axial vein are spatially juxtaposed, the initial angiogenic sprouts from these vessels extend in opposite directions, indicating that distinct cues may regulate angiogenesis of the axial vessels. We found that angiogenic sprouts from the dorsal aorta are dependent on vascular endothelial growth factor A (Vegf-A) signalling, and do not respond to bone morphogenetic protein (Bmp) signals. In contrast, sprouts from the axial vein are regulated by Bmp signalling independently of Vegf-A signals, indicating that Bmp is a vein-specific angiogenic cue during early vascular development. Our results support a paradigm whereby different signals regulate distinct programmes of sprouting angiogenesis from the axial vein and dorsal aorta, and indicate that signalling heterogeneity contributes to the complexity of vascular networks.

The dorsal aorta and axial vein form a primitive circulatory loop, and subsequent angiogenesis from these vessels is essential to generate the complex vascular networks found in vertebrates. In zebrafish, the initial sprouts from the dorsal aorta project dorsally to form the intersegmental arteries[1] (ISAs; Supplementary Fig. S1a, arrows), whereas those from the posterior axial vein extend ventrally (Supplementary Fig. S1a, arrowheads) to form a honeycomb-like network termed the caudal vein plexus (CVP), which is composed of a dorsal and ventral vein with interconnecting vessels (Supplementary Fig. S1a). As the neighbouring axial vessels extend angiogenic sprouts in opposite directions and form distinct vascular networks, we formed a hypothesis that the dorsal aorta and axial vein respond to different angiogenic stimuli.

As the Vegf-A signalling cascade is a critical angiogenic stimulus for many vascular beds[2], we assessed the role of Vegf-A in regulating sprouting angiogenesis from the axial vessels. Co-injection of morpholino oligonucleotides against two Vegf-A receptors in zebrafish, *kdrl* and *kdr* (ref. 3), caused severe vascular defects. The dorsal aorta and the caudal vein segregated incompletely[4] (Fig. 1a), the level of endothelial cell apoptosis was significantly increased[5] (Supplementary Fig. S1b) and the formation of ISA sprouts was blocked[5] (Fig. 1a). Whereas the percentage of segments (the area defined by two adjacent somite boundaries) containing an ISA was markedly reduced, the percentage containing a CVP was largely unaffected in *kdrl*/*kdr* morphants (Fig. 1b; see Methods for quantification details). The venous sprouts still formed a primitive plexus in *kdrl*/*kdr* morphants, and had only marginal defects in branching (Fig. 1 and Supplementary Fig. S1c). This vascular network was unstable and ultimately regressed, as previously reported[4]. Although our data corroborate the role of Vegf-A signalling in regulating ISA formation and endothelial cell stability[3], they indicate that another angiogenic stimulus regulates sprouting from the axial vein.

To identify the angiogenic signal required for sprouting from the axial vein, we analysed the expression of components from several signalling pathways (data not shown), and found that Bmp pathway components were selectively expressed in the developing CVP. Whole-mount *in situ* hybridization indicated that the *bmp2b* ligand was expressed at high levels within the CVP and surrounding tissue during plexus formation (26–32 h post-fertilization (hpf)), and expression subsided as the CVP stabilized at 38 hpf (Fig. 1c and Supplementary Fig. S1d). Furthermore, two Bmp type II receptors, *bmpr2a* and *bmpr2b*, were expressed at high levels in the endothelial cells of the CVP at 26, 32 and 38 hpf, consistent with previous studies[6] (Fig. 1c and Supplementary Fig. S1d).

Bmp can function as a context-dependent pro-angiogenic cue[7]. Following ligand binding, Bmp type II receptors phosphorylate Bmp

[1]Department of Biology, University of North Carolina at Chapel Hill, Chapel Hill, North Carolina 27599, USA. [2]Department of Internal Medicine, Section of Cardiovascular Medicine, Yale University Medical School, New Haven, Connecticut 06511, USA. [3]Division of Cardiovascular Medicine, Department of Medicine, Department of Pharmacology, Vanderbilt University School of Medicine, Nashville, Tennessee 37232, USA. [4]Research Medicine, Veterans Affairs TVHS, Nashville, Tennessee 37212, USA. [5]McAllister Heart Institute, University of North Carolina at Chapel Hill, Chapel Hill, North Carolina 27599, USA. [6]Department of Cell and Molecular Physiology, University of North Carolina at Chapel Hill, Chapel Hill, North Carolina 27599, USA. [7]Present address: Department of Internal Medicine, Section of Cardiovascular Medicine, Yale University Medical School, New Haven, Connecticut 06511, USA.
[8]Correspondence should be addressed to S-W.J. or V.L.B. (e-mail: suk-won.jin@yale.edu or bautch@med.unc.edu)

Received 8 April 2010; accepted 8 March 2011; published online 15 May 2011; DOI: 10.1038/ncb2232

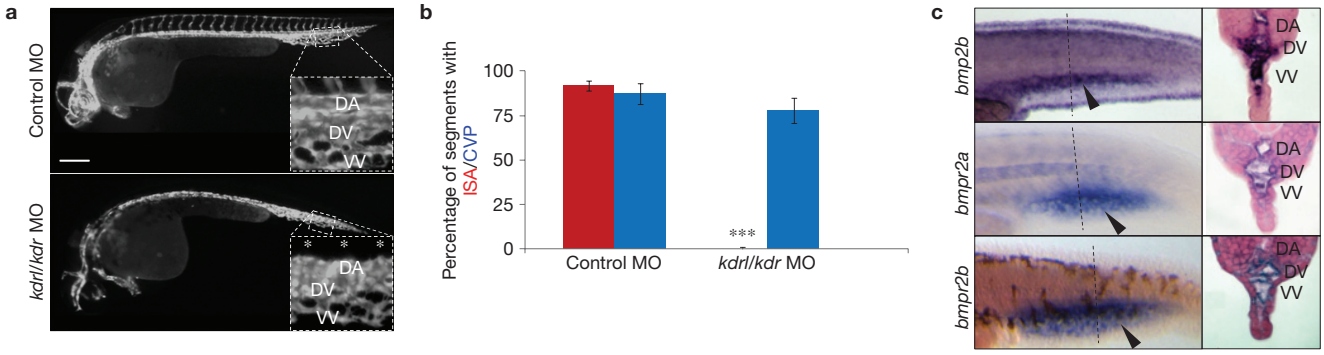

Figure 1 The axial vein forms angiogenic sprouts despite loss of Vegf receptor activity, and expresses Bmp pathway components. (**a**) Epifluorescence micrographs of 34-hpf *Tg(kdrl:GFP)* control embryos and embryos injected with *kdrl*/*kdr* morpholino oligonucleotides (MOs); insets show a higher magnification of the CVP region. Asterisks denote the lack of intersegmental arteries in embryos injected with *kdrl*/*kdr* morpholino oligonucleotides. Scale bar, 250 μm. (**b**) The percentage of segments that contain an ISA (red bars) or a CVP (blue bars) in control embryos ($n = 9$) and embryos injected with *kdrl*/*kdr* morpholino oligonucleotides ($n = 10$). *kdrl*/*kdr* morpholino oligonucleotides completely blocked the formation of arteries but not veins. Error bars represent mean ± s.e.m. $^{***}P < 0.001$ versus control, Student's *t*-test. (**c**) Expression pattern of *bmp2b*, *bmpr2a* and *bmpr2b* in the developing CVP region (black arrowheads) at 32 hpf, as detected by *in situ* hybridization. Cross-sections from different 32-hpf embryos were taken at the area marked by the dashed line. DA, dorsal aorta; VV, ventral vein; DV, dorsal vein.

type I receptors, which in turn activate Smad and/or mitogen-activated protein (MAP) kinase signalling[8]. To test whether Bmp signalling regulates sprouting of the axial vein, we manipulated expression of Bmp pathway components in the developing zebrafish using a heat-shock promoter (*hsp70l*; ref. 9). To determine the expression profile of *hsp70l*, we heat-shocked *Tg(hsp70l:GFP)* embryos at 25 hpf and found that GFP (green fluorescent protein) was expressed in most tissues and cell types (Supplementary Fig. S2a). We analysed the effects of decreased Bmp activity on sprouting from the axial vein by overexpressing *noggin3*, an endogenous inhibitor of Bmp signalling[10]. Control embryos heat-shocked at the onset of plexus formation (25 hpf) showed no apparent vascular abnormalities (Fig. 2a and Supplementary Movie S1). In contrast, heat-shocked *Tg(hsp70l:noggin3)* embryos had a CVP with aberrant sprouts that failed to make proper connections with neighbouring sprouts, but showed no ISA defects (Fig. 2a, arrows, Supplementary Fig. S3a and Supplementary Movie S2). Similar results were also observed in *Tg(hsp70l:dnbmprI–GFP)* embryos that expressed a dominant-negative Bmp receptor type I–GFP fusion construct (DNBmprI–GFP) when heat-shocked (Supplementary Fig. S2b). As CVP patterning was perturbed while ISA patterning was largely unaffected, these results indicate that decreased Bmp signalling selectively affects vessel patterning from the axial vein.

We investigated whether increased Bmp signalling could induce angiogenesis. The level of *bmp2b* expression was increased in heat-shock-treated *Tg(hsp70l:bmp2b)* embryos at the onset of CVP formation. Overexpression of *bmp2b* induced ectopic sprouts along the axial vein, with the most robust ectopic sprouting occurring in the CVP (Fig. 2a, arrowheads, Supplementary Fig. S3b and Supplementary Movie S3). Bmp-induced ectopic sprouts extended from the axial vein and migrated between the epithelial surface and the somite boundary, forming an additional plexus in a region that is avascular in wild-type embryos (Supplementary Fig. S4a, arrowheads). The Bmp-induced plexus expressed a venous marker gene, *disabled homologue 2* (*dab2*), at high levels, indicating that it has a venous identity (Supplementary Fig. S4b). Although Bmp overexpression induced robust sprouting from the axial vein, ectopic sprouts were never observed from the dorsal aorta (Fig. 2a). To further delineate the specificity of Bmp signalling, wild-type and *Tg(hsp70l:bmp2b)* embryos were heat-shocked at 2.5 days post-fertilization, when ventral sprouts from the axial vein form the subintestinal vein plexus (SIVP) (Supplementary Fig. S4c, arrows). The SIVP in embryos overexpressing *bmp2b* was shifted dorsally (Supplementary Fig. S4c, arrows) and contained ectopic vessels (Supplementary Fig. S4c, arrowhead), indicating that the SIVP is also responsive to Bmp signalling. These data indicate that sprouting angiogenesis from the axial vein during early development is uniquely dependent on Bmp signalling.

To assess the cellular effects of Bmp signalling on venous endothelial cell behaviour, we carried out time-lapse imaging. Wild-type embryos formed a honeycomb-like plexus by 32 hpf, and this plexus began to retract filopodia and stabilize by 35 hpf (Fig. 2b and Supplementary Movie S1). However, *Tg(hsp70l:noggin3)* embryos contained atypical angiogenic sprouts that failed to make connections and never formed a proper plexus (Fig. 2b and Supplementary Movie S2). In contrast, *Tg(hsp70l:bmp2b)* embryos contained ectopic endothelial sprouts. These ectopic sprouts branched and sprouted from the dorsal vein of the CVP as early as 6.5 h after heat-shock treatment (32 hpf) and rapidly migrated dorsally (Fig. 2b and Supplementary Movie S3).

To better characterize the *noggin3*- and *bmp2b*-overexpression phenotypes, we counted venous endothelial cell nuclei and carried out branch-point analyses in wild-type, *noggin3*- and *bmp2b*-overexpressing embryos. Whereas the number of venous endothelial cells in the CVP remained relatively unchanged in *noggin3*-overexpressing embryos, we observed a slight but significant increase in endothelial cell numbers in *bmp2b*-overexpressing embryos (Supplementary Fig S3c). Venous branch points, however, were significantly altered in both *noggin3*- and *bmp2b*-overexpressing embryos (Supplementary Fig. S3d). The number of branch points was decreased more than 7-fold by *noggin3* overexpression, and increased approximately 2.5-fold by *bmp2b* overexpression (Supplementary Fig. S3d). Overexpression of *bmp2b* also caused a significant increase in the number of filopodia (Supplementary Fig. S4d–e), and randomized their direction of extension (Supplementary Fig. S4f). Taken together, our data indicate that Bmp is a pro-angiogenic cue that regulates angiogenesis in the axial vein.

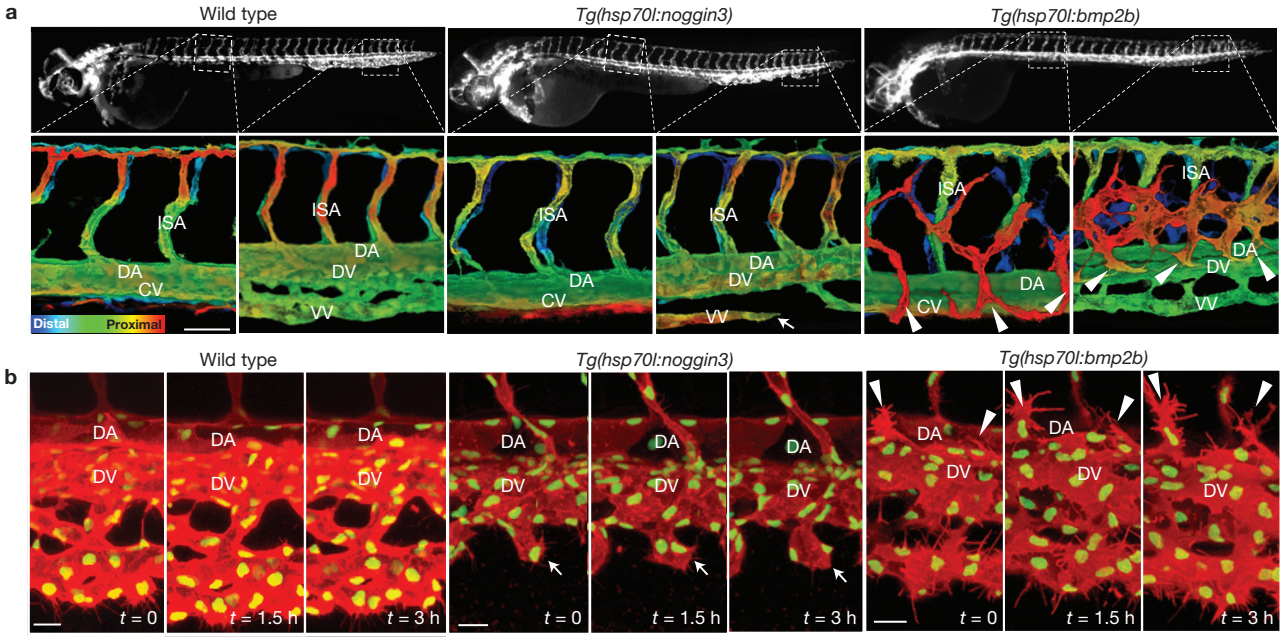

Figure 2 Bmp signalling is necessary and sufficient for sprouting from the axial vein. (**a**) Blood vessels in wild-type, *Tg(hsp70:noggin3)* and *Tg(hsp70:bmp2b)* embryos in the *Tg(kdrl:GFP)* transgenic background. The entire vascular network of 42-hpf embryos was analysed using epifluorescence micrographs; dashed squares represent the trunk and tail areas analysed below. *Z* stacks from the trunk and tail regions were used to make 3D colour projections, where red represents the most proximal (closest to viewer) and blue represents the most distal (farthest from viewer) blood vessels (epifluorescence micrographs and 3D colour projections were taken from different embryos). Scale bar, 50 μm. (**b**) Time-lapse imaging of *Tg(fli1:nGFP);Tg(kdrl:ras–mCherry)* embryos starting at 32 hpf. Arrows in **a** and **b** show sprouts from the axial vein that fail to make connections in *Tg(hsp70:noggin3)* embryos. Arrowheads in **a** and **b** point to ectopic sprouts that branch from the axial vein in *Tg(hsp70:bmp2b)* embryos. Scale bars, 20 μm. DA, dorsal aorta; VV, ventral vein; DV, dorsal vein; ISA, intersegmental artery.

To investigate whether the Bmp type II receptors expressed in the developing CVP regulate Bmp-mediated angiogenesis, we analysed *bmpr2a* or *bmpr2b* morphants (Fig. 3a–d and Supplementary Fig. S5). Whereas the number of arterial sprouts did not differ significantly from control embryos, sprouts from the axial vein were significantly reduced in number in *bmpr2a* and *bmpr2b* morphants (Fig. 3a,b and Supplementary Fig. S5c). Moreover, knockdown of *bmpr2a* or *bmpr2b* in *bmp2b*-overexpressing embryos inhibited the formation of ectopic sprouts (Fig. 3c,d and Supplementary Fig. S5d). Therefore, Bmpr2a and Bmpr2b regulate Bmp-mediated angiogenesis from the axial vein.

Considering the expression and function of *bmpr2a* and *bmpr2b* in CVP formation, it is likely that Bmp activation is required in endothelial cells. To investigate this hypothesis, we generated mosaic embryos by injecting either *kdrl:GFP* or *kdrl:DNBmprI–GFP* in the *Tg(kdrl:mCherry)* background. The resulting embryos contained patches of endothelial cells that strongly expressed *GFP* or *DNBmprI–GFP*. The *GFP*-expressing control cells extended venous sprouts, which made connections and formed a honeycomb-like plexus (Fig. 3e and Supplementary Movie S4). In contrast, the *DNBmprI–GFP*-expressing cells were unable to extend sprouts from the axial vein, and they failed to connect with neighbouring endothelial cells to form a honeycomb-like plexus (Fig. 3f and Supplementary Movie S5).

The segments that contained *DNBmprI–GFP*-expressing cells had fewer branch points than *GFP*-expressing control cells (Fig. 3g), indicating that Bmp signalling within endothelial cells is important during branching morphogenesis. Furthermore, the frequency with which the branches connected to form a plexus was significantly reduced in *DNBmprI–GFP*-expressing cells, indicating that Bmp signalling within endothelial cells is critical for the formation of endothelial networks (Fig. 3h). Taken together, our results indicate that Bmp-mediated angiogenesis requires Bmp activation in endothelial cells.

Bmp signalling activates the Smad signalling cascade and/or alternative MAP kinase signalling cascades such as the extracellular signal-regulated kinase (Erk) and p38 cascades[11,12]. To delineate the downstream factors critical for Bmp-mediated angiogenesis, we analysed the activity/phosphorylation status of Smad1/5/8 (R-Smads) and Erk. Activated R-Smads and Erk were present within the ectopic sprouts from the axial vein (Supplementary Fig. S6a,b). To assess the function of R-Smad and Erk signalling in Bmp-mediated angiogenesis, we blocked the activity of R-Smad or Erk by treating embryos with small-molecule inhibitors. To inhibit the R-Smad signalling cascade, we used 4-(6-(4-isopropoxyphenyl)pyrazolo[1,5-a]pyrimidin-3-yl)quinoline (DMH1), which inhibits activin receptor-like kinase 2/3 (Alk2/3) and selectively abrogates activation of R-Smads without affecting MAP kinase activity[13]. We also inhibited the p38 pathway with SB203580, and the Erk pathway with either U0126 (data not shown) or SL327. Whereas arterial and venous angiogenesis was unaffected by treatment with dimethylsulphoxide (DMSO) or the p38 inhibitor, inhibition of R-Smad activation selectively blocked the formation of the CVP without affecting ISAs, and inhibition of Erk activity blocked the formation of both the CVP and ISAs (Fig. 4a,b). Moreover, inhibiting R-Smad or Erk activation in Bmp-overexpressing embryos efficiently inhibited the percentage of segments with ectopic vessels, whereas p38 inhibition had no effect on the percentage of segments with ectopic vessels (Fig. 4c,d). Interestingly, the Erk inhibitor also markedly attenuated the length and progression of the ectopic sprouts (Fig. 4e).

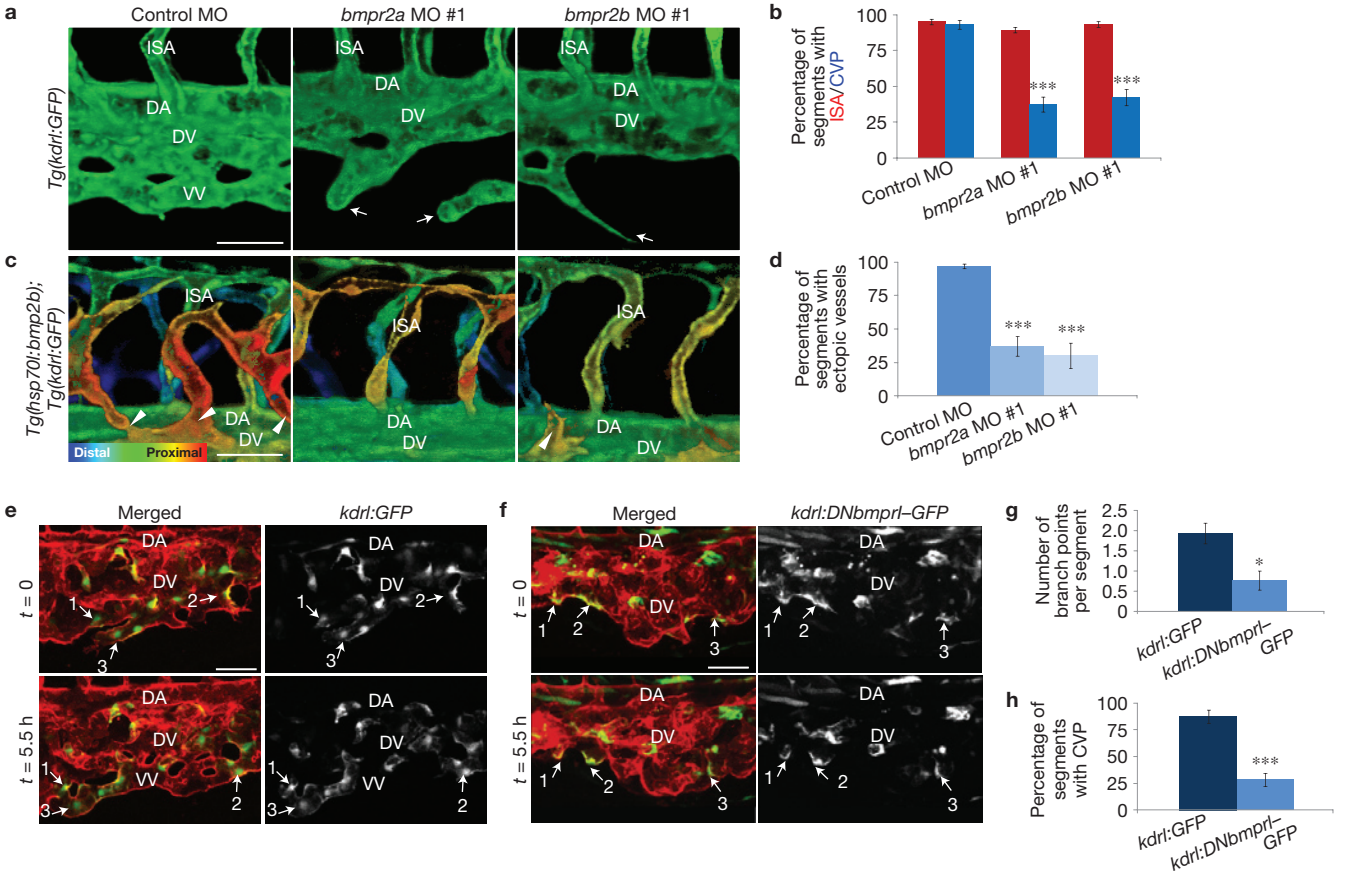

Figure 3 Angiogenesis from the axial vein requires *bmpr2a* and *bmpr2b* and involves endothelial cell autonomous activation of Bmp signalling. (**a**) Confocal monochrome projections of *Tg(kdrl:GFP)* embryos injected with a standard control, *bmpr2a* or *bmpr2b* morpholino oligonucleotides (MOs). The sprouts from the axial vein are disrupted with *bmpr2a* and *bmpr2b* morpholino oligonucleotides (arrows). (**b**) The percentage of segments that contain an ISA (red bars) or a CVP (blue bars). Eight embryos were used for the quantification in each case. *bmpr2a* or *bmpr2b* morpholino oligonucleotides blocked the formation of veins but not arteries. (**c**) Depth colour-coded projections of confocal micrographs of *Tg(hsp70l:bmp2b);Tg(kdrl:GFP)* heat-shocked embryos injected with a standard control, *bmpr2a* or *bmpr2b* morpholino oligonucleotides. The ectopic sprouts (arrowheads) are reduced in both *bmpr2a* and *bmpr2b* morphants. (**d**) The percentage of segments that contain an ectopic sprout in control embryos ($n = 37$), embryos injected with *bmpr2a* morpholino #1 ($n = 27$) and embryos injected with *bmpr2b* morpholino #1 ($n = 15$). The number of Bmp-induced ectopic sprouts was significantly reduced in both *bmpr2a* and *bmpr2b* morphants. (**e**,**f**) Time-lapse confocal images of *Tg(kdrl:GFP)* (**e**) and *Tg(kdrl:DNBmpr1–GFP)* (**f**) mosaic embryos in a *Tg(kdrl:ras-mCherry)* background. Numbered arrows indicate mosaic endothelial cells. (**g**,**h**) The number of branch points (**g**) and the percentage of segments containing a CVP (**h**) in mosaic segments containing *GFP* or *DNBmprl–GFP* cells. For quantification (see Methods), 29 segments in 7 embryos were used for *Tg(kdrl:GFP)* and 34 segments in 11 embryos were used for *Tg(kdrl:DNBmpr1–GFP)*. *DNBmprl–GFP*-expressing endothelial cells contain fewer branches (**g**) and fail to form proper CVP connections (**h**). Scale bar, 50 μm. Error bars represent mean ± s.e.m. $^{**}P < 0.01$ and $^{***}P < 0.001$ versus control, Student's *t*-test. DA, dorsal aorta; ISA, intersegmental artery; VV, ventral vein; DV, dorsal vein.

Collectively, these results indicate that R-Smad activation selectively regulates venous sprouting angiogenesis, and Erk (but not p38) activation is involved in the progression of Bmp-mediated venous sprouts as well as arterial sprouts.

As activation of the Bmp signalling cascade transcriptionally regulates multiple genes and pathways, we analysed the transcriptional levels of important regulators of angiogenesis using quantitative real-time PCR. Transcription levels of *Tg(hsp70l:bmp2b)* embryos were compared with wild-type embryos 2 and 5 h after heat-shock induction of *bmp2b* expression. A downstream transcriptional target of Bmp signalling, *id2a* (*inhibitor of DNA binding 2, dominant-negative helix–loop–helix protein, a*), was used as a positive control. The genes *vegfa*, *vegfc* (also a major stimulus of lymphangiogenesis[14]), *vegfr3* (also known as *flt4*; a venous marker and receptor for Vegf-C) and *delta-like protein 4* (*dll4*; an arterial marker and tip cell marker[15,16]) were also tested. Bmp overexpression upregulated *id2a* by over threefold 2 h after heat-shock treatment, whereas *vegfa*, *vegfc*, *flt4* and *dll4* were either marginally affected or not affected at all (Supplementary Fig. S7). Furthermore, *vegfa*, *vegfc*, *flt4* and *dll4* transcript levels were unaffected 5 h after heat-shock induction of *bmp2b* expression (Supplementary Fig. S7).

To test the physiological relevance of the moderate increase in *vegfa* transcription at 2 h post-heat-shock, Bmp overexpression was induced in embryos lacking Vegf receptors. Co-injection of the *kdrl*/*kdr* morpholino oligonucleotides resulted in the formation of a single axial vein at 2 days post-fertilization (Fig. 5a). Despite the severely disrupted vascular network, Bmp-induced ectopic blood vessel formation was unaffected in *kdrl*/*kdr* morphants, demonstrating that Bmp is capable of inducing angiogenesis when Vegf signalling is

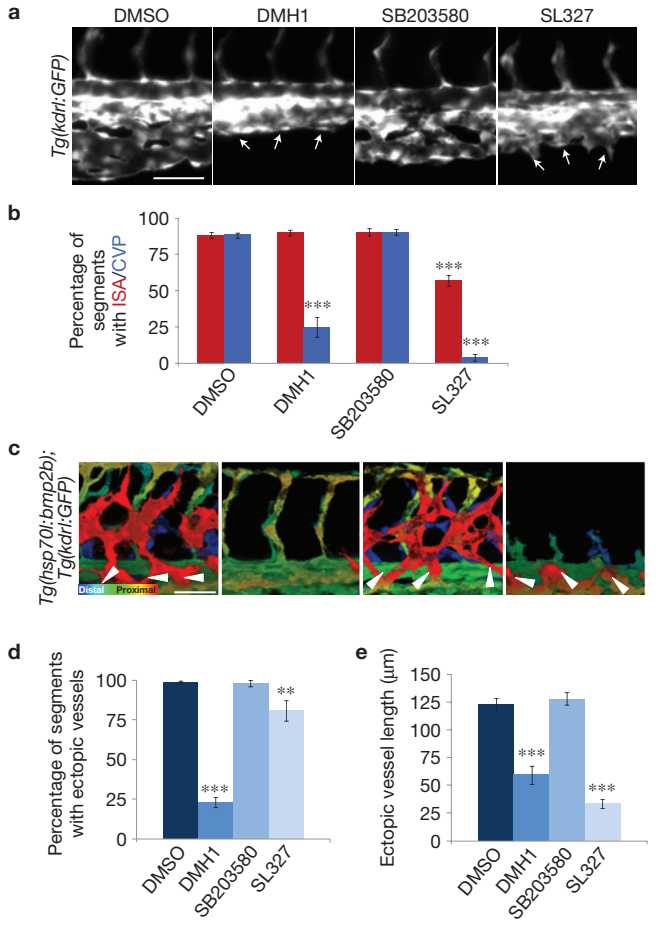

Figure 4 Activation of R-Smad and Erk mediates Bmp-induced angiogenesis. (**a**) Epifluorescence micrographs of *Tg(kdrl:GFP)* 38-hpf embryos treated with DMSO, DMH1 (R-Smad inhibitor), SB203580 (p38 inhibitor) and SL327 (Erk inhibitor). Arrows point to defects in the formation of venous vessels in DMH1- or SL327-treated embryos. (**b**) The percentage of segments that contain an ISA (red bars) or a CVP (blue bars) in embryos treated with DMSO ($n = 14$), DMH1 ($n = 13$), SB203580 ($n = 8$) or SL327 ($n = 10$). (**c**) Depth colour-coded projections of confocal micrographs of *Tg(hsp70l:bmp2b);Tg(kdrl:GFP)* 46-hpf embryos taken after treatment with small-molecule inhibitors. Addition of DMH1 or SL327 to *bmp2b*-overexpressing embryos inhibited Bmp-induced ectopic sprouts. Arrowheads point to ectopic sprouts from the axial vein. (**d**) The percentage of segments that contain an ectopic vessel in embryos treated with DMSO ($n = 11$), DMH1 ($n = 13$), SB203580 ($n = 4$) or SL327 ($n = 6$). (**e**) The average ectopic vessel length in embryos treated with DMSO ($n = 15$), DMH1 ($n = 14$), SB203580 ($n = 16$) or SL327 ($n = 22$). Inhibition of either R-Smad or Erk activation significantly reduced the formation and average length of ectopic vessels. Error bars represent mean ± s.e.m. $^{**}P < 0.01$ and $^{***}P < 0.001$ versus control, Student's *t*-test.

inhibited (Fig. 5a,b). We next analysed the effects of Bmp and Vegf-A small-molecule inhibitors during sprouting angiogenesis of the axial vessels[12]. The addition of dorsomorphin, a chemical inhibitor of both the Bmp and Vegf-A signalling pathways, effectively inhibited the formation of angiogenic vessels from the dorsal aorta and axial vein, and blocked Bmp-induced ectopic vessel formation (Supplementary Fig. S8). DMH4, an inhibitor of Vegf-A signalling, preferentially blocked the formation of vessels from the dorsal aorta and had no effect on Bmp-induced ectopic vessel formation, whereas DMH1, an inhibitor of Bmp signalling, selectively inhibited the formation of vessels from the axial vein and disrupted Bmp-induced ectopic vessel formation (Supplementary Fig. S8). Taken together, these findings demonstrate that Bmp is the main stimulus for sprouting angiogenesis from the axial vein, and that Vegf-A is the main stimulus for sprouting from the dorsal aorta. Moreover, these results indicate that Bmp mediates angiogenesis independently of a significant contribution from Vegf-A signalling.

To compare the angiogenic effects of Bmp and Vegf-A, we induced overexpression of *bmp2b* or $vegfa_{121}$ by heat-shock treatment of *Tg(hsp70l:bmp2b)* or *Tg(hsp70l:*$vegfa_{121}$*)* transgenic lines, respectively. As expected, *bmp2b* overexpression induced the formation of robust ectopic sprouts along the axial vein, but not from the dorsal aorta (Fig. 5c). In contrast, $vegfa_{121}$ overexpression did not induce the formation of ectopic sprouts from the axial vein, but increased sprouting along the dorsal aorta (Fig. 5c). The distinct angiogenic responses between *bmp2b*-overexpressing embryos and $vegfa_{121}$-overexpressing embryos demonstrate that Bmp is a distinct and potent pro-angiogenic factor.

Taken together, our findings support a paradigm whereby Bmp signalling mediates venous angiogenesis, whereas Vegf-A signalling directs arterial angiogenesis. In our model, this differential response to angiogenic stimuli permits neighbouring venous and arterial vessels to extend distinct angiogenic sprouts and form non-overlapping vascular networks (Fig. 5d). The venous sensitivity observed during Bmp-mediated angiogenesis may be provided by the notochord, which lies above the dorsal aorta and expresses Bmp antagonists that inhibit blood vessel growth[17,18]. Collectively, our results support a model of Bmp-mediated angiogenesis in which Bmp2b binds Bmpr2a/b and Alk2/Alk3 hetero-tetrameric receptor complexes in venous endothelial cells and activates R-Smad and Erk, which elicits angiogenic responses that include sprout migration and fusion (Fig. 5e).

The zebrafish embryo contains a relatively simple and streamlined vascular system, and this simplicity allows for elucidation of binary choices that probably underlie vascular development in more complex organisms. It will be important to determine whether there is a similar role for Bmp signalling during mammalian development and tumour angiogenesis. Although published work in mammalian systems does not identify a selective requirement for Bmp signalling in venous angiogenesis, mammalian vascular systems are more complex, and the requirement for BMP signalling in early development makes specific interrogation of later requirements difficult[19–22]. Furthermore, several types of carcinoma express high levels of BMP growth factors[23–25], and anti-angiogenesis cancer drugs that singularly antagonize VEGF-A activity are only partially effective[26]. Therefore, future studies that target both Bmp and Vegf-A signalling may be more successful at manipulating blood vessel growth. □

METHODS

Methods and any associated references are available in the online version of the paper at http://www.nature.com/naturecellbiology

Note: Supplementary Information is available on the Nature Cell Biology website

ACKNOWLEDGEMENTS

The authors thank E. Flynn for excellent fish care; the members of the Jin and Bautch laboratories for discussions; the UNC Histology Facility; Michael Hooker Microscopy Facility; W. Comb and M. Aleman for technical assistance; and M. Hammerschmidt and N. Chi for providing transgenic lines, and C-B. Chien for the *kdrl* 5′ entry gateway vector. The authors also thank F. Conlon, M. Majesky, C. Patterson and J. Rawls for discussion and critical reading of the manuscript.

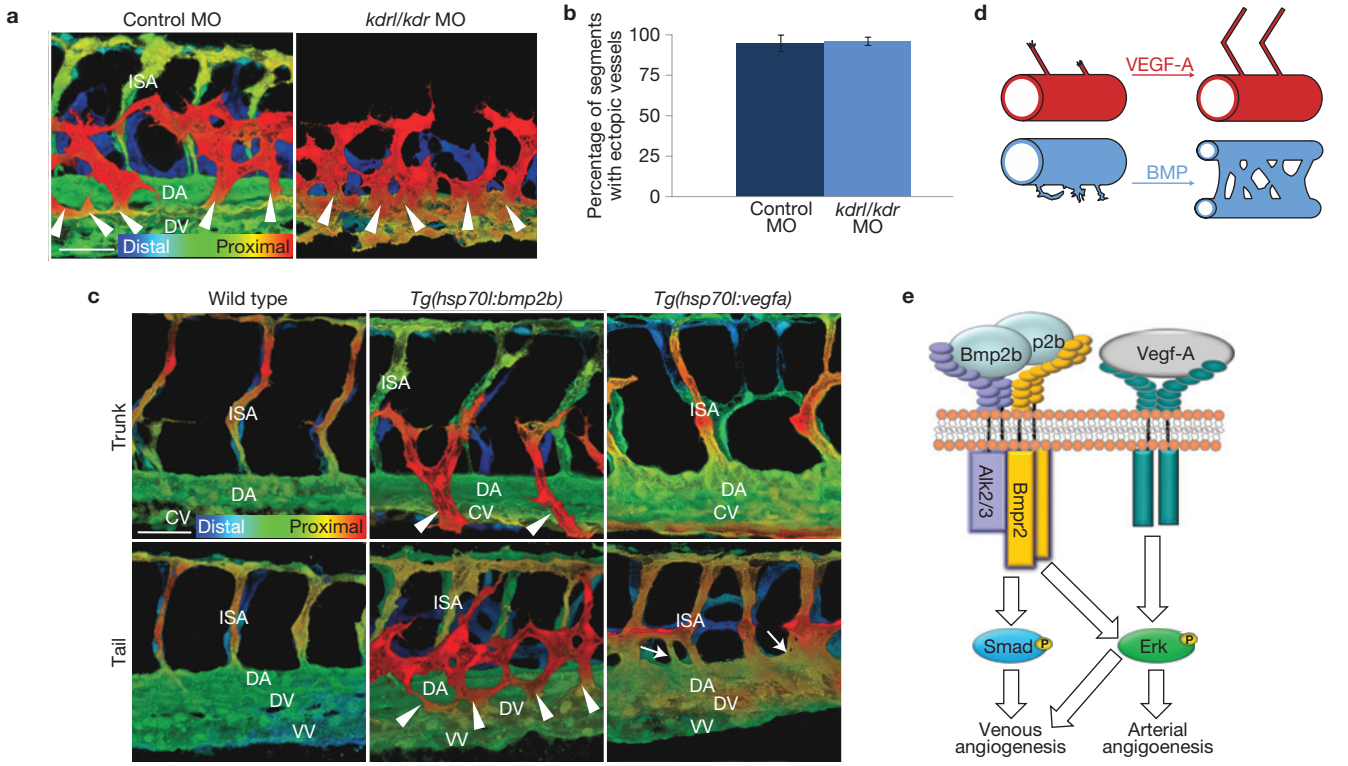

Figure 5 Bmp signalling regulates axial vein angiogenesis independently of Vegf receptor activity. (**a**) Three-dimensional colour projections of *Tg(hsp70:bmp2b);Tg(kdrl:GFP)* heat-shocked embryos injected with control and *kdrl/kdr* morpholino oligonucleotides (MOs). The number of Bmp-induced ectopic sprouts (arrowheads) was not affected by the loss of Kdrl/Kdr activity. Scale bar, 50 μm. (**b**) The percentage of segments that contain ectopic vessels ($n = 3$ for control, and 6 for *kdrl/kdr* morpholino oligonucleotides). There was no statistically significant difference between control embryos and embryos injected with *kdrl/kdr* morpholino oligonucleotides. Error bars represent mean ± s.e.m. (**c**) Three-dimensional colour projections from the trunk and tail region of 42-hpf heat-shocked embryos. Overexpression of *bmp2b* induced ectopic sprouts in venous endothelial cells (arrowheads), whereas overexpression of *vegfa* stimulated ectopic sprouts in arterial endothelial cells in the trunk (arrows). (**d**) In this model, Bmp signalling is the dominant regulator of axial vein angiogenesis, whereas Vegf-A is the main regulator of angiogenesis from the dorsal aorta. (**e**) In venous endothelial cells, the Bmp2b ligand binds to a Bmpr2a and/or Bmpr2b and Alk2/Alk3 hetero-tetrameric complex, which phosphorylates R-Smad and Erk to promote angiogenesis, whereas arterial cells use the classical Vegf-A signalling cascade to induce angiogenesis. Scale bar, 50 μm. DA, dorsal aorta; VV, ventral vein; DV, dorsal vein; ISA, intersegmental artery.

This study was supported by grants from the NIH to S-W.J. (HL090960) and V.L.B. (HL43174 and HL86564), and the UNC Integrative Vascular Biology Training Grant (T32HL69768) and an American Heart Association Pre-doctoral Fellowship to D.M.W.

AUTHOR CONTRIBUTIONS

D.M.W., V.L.B. and S-W.J. designed the experiments, D.M.W. carried out the experiments, J-D.K. helped with *in situ* hybridization, J.H. and C.C.H. provided key reagents and D.M.W., V.L.B. and S-W.J. wrote the manuscript.

COMPETING FINANCIAL INTERESTS

The authors declare no competing financial interests.

Published online at http://www.nature.com/naturecellbiology
Reprints and permissions information is available online at http://www.nature.com/reprints

1. Isogai, S., Lawson, N., Torrealday, S., Horiguchi, M. & Weinstein, B. Angiogenic network formation in the developing vertebrate trunk. *Development* **130,** 5281–5290 (2003).
2. Risau, W. Mechanisms of angiogenesis. *Nature* **386,** 671–674 (1997).
3. Covassin, L., Villefranc, J., Kacergis, M., Weinstein, B. & Lawson, N. Distinct genetic interactions between multiple Vegf receptors are required for development of different blood vessel types in zebrafish. *Proc. Natl Acad. Sci. USA* **103,** 6554–6559 (2006).
4. Herbert, S. *et al.* Arterial-venous segregation by selective cell sprouting: an alternative mode of blood vessel formation. *Science* **326,** 294–298 (2009).
5. Lee, S. *et al.* Autocrine VEGF signalling is required for vascular homeostasis. *Cell* **130,** 691–703 (2007).
6. Monteiro, R. *et al.* Two novel type II receptors mediate BMP signalling and are required to establish left-right asymmetry in zebrafish. *Dev. Biol.* **315,** 55–71 (2008).
7. Langenfeld, E. M. & Langenfeld, J. Bone morphogenetic protein-2 stimulates angiogenesis in developing tumours. *Mol. Cancer Res.* **2,** 141–149 (2004).
8. Sieber, C., Kopf, J., Hiepen, C. & Knaus, P. Recent advances in BMP receptor signalling. *Cytokine Growth Factor Rev.* **20,** 343–355 (2009).
9. Halloran, M.C. *et al.* Laser-induced gene expression in specific cells of transgenic zebrafish. *Development* **127,** 1953–1960 (2000).
10. Fürthauer, M., Thisse, B. & Thisse, C. Three different noggin genes antagonize the activity of bone morphogenetic proteins in the zebrafish embryo. *Dev. Biol.* **214,** 181–196 (1999).
11. Derynck, R. & Zhang, Y. Smad-dependent and Smad-independent pathways in TGF-B family signalling. *Nature* **425,** 577–584 (2003).
12. Pi, X. *et al.* Sequential roles for myosin-X in BMP6-dependent filopodial extension, migration, and activation of BMP receptors. *J. Cell Biol.* **179,** 1569–1582 (2007).
13. Hao, J. *et al. In vivo* structure–activity relationship study of dorsomorphin analogues identifies selective VEGF and BMP inhibitors. *ACS Chem. Biol.* **19,** 245–253 (2010).
14. Jeltsch, M. *et al.* Hyperplasia of lymphatic vessels in VEGF-C transgenic mice. *Science* **276,** 1423–1425 (1997).
15. Hellström, M. *et al.* Dll4 signalling through Notch1 regulates formation of tip cells during angiogenesis. *Nature* **445,** 776–780 (2007).
16. Siekmann, A. F. & Lawson, N. D. Notch signalling limits angiogenic cell behaviour in developing zebrafish arteries. *Nature* **445,** 781–4 (2007).
17. Reese, D. E., Hall, C. E. & Mikawa, T. Negative regulation of midline vascular development by the notochord. *Dev. Cell* **6,** 699–708 (2004).
18. Bressan, M., Davis, P., Timmer, J., Herzlinger, D. & Mikawa, T. Notochord-derived BMP antagonists inhibit endothelial cell generation and network formation. *Dev. Biol.* **326,** 101–111 (2009).

19. Gu, Z. *et al*. The type I serine/threonine kinase receptor ActRIA (ALK2) is required for gastrulation of the mouse embryo. *Development* **126,** 2551–61 (1999).
20. Mishina, Y., Crombie, R., Bradley, A. & Behringer, R. R. Multiple roles for activin-like kinase-2 signalling during mouse embryogenesis. *Dev. Biol.* **213,** 314–26 (1999).
21. Beppu, H. *et al*. BMP type II receptor is required for gastrulation and early development of mouse embryos. *Dev. Biol.* **221,** 49–58 (2000).
22. Hong, K. H. *et al*. Genetic ablation of the BMPR2 gene in pulmonary endothelium is sufficient to predispose to pulmonary arterial hypertension. *Circulation* **118,** 722–730 (2008).
23. Kleeff, J. *et al*. Bone morphogenetic protein 2 exerts diverse effects on cell growth in vitro and is expressed in human pancreatic cancer *in vivo*. *Gastroenterology* **116,** 1202–1216 (1999).
24. Jin, Y. *et al*. Overexpression of BMP-2/4, -5 and BMPR-IA associated with malignancy of oral epithelium. *Oral Oncol*. **37,** 225–233 (2001).
25. Langenfeld, E. M. *et al*. The mature bone morphogenetic protein-2 is aberrantly expressed in non-small cell lung carcinomas and stimulates tumour growth of A549 cells. *Carcinogenesis* **24,** 1445–1454 (2003).
26. Ferrara, N. & Kerbel, R. S. Angiogenesis as a therapeutic target. *Nature* **438,** 967–974 (2005).

METHODS

Zebrafish husbandry. Zebrafish (*Danio rerio*) embryos were raised as previously described[27]. The following transgenic lines were used: *Tg*(*fli1*:*nEGFP*)^{y7} (ref. 28), *Tg*(*kdrl*:*GFP*)^{s843} (ref. 29), *Tg*(*kdrl*:*ras–mCherry*)^{s896} (ref. 30), *Tg*(*hsp70l*:*bmp2b*)^{fr13} (ref. 31), *Tg*(*hsp70l*:*noggin*)^{fr13} (ref. 31), *Tg*(*hsp70l*:*dnbmprI–GFP*)^{w30} (ref. 32) and *Tg*(*hsp70l*:*vegfaa*$_{121}$;*cmlc2*:*EGFP*)^{nc2} (this study).

***In situ* hybridization and immunohistochemistry.** Whole-mount *in situ* hybridization was carried out as previously described[33,34]. Probes for *bmp2b*, *bmpr2a*, *bmpr2b* and *dab2* were synthesized as previously described[6], and documented with a Leica MF16 microscope. For transverse sections, embryos were mounted in 4% agarose, embedded in paraffin, and sectioned into 8, 7 and 5 μm slices respectively. Fast red staining was used to visualize tissue morphology.

Immunohistochemistry was carried out as previously described[29]. The following antibodies were used: anti-Caspase3, cleaved (Cat no:PC679, Calbiochem), β-tubulin (Cat no:61053, BD Transduction Laboratories) at 1:200, and Alexa Fluor secondary antibodies (Invitrogen) at 1:400. To sagittally mount embryos, the head and yolk were removed and the trunk was covered in 1% low-melt agarose and sealed with a cover slip. For transverse sections, embryos were mounted in 4% agarose and sectioned on a Leica VT 1000s vibratome.

Heat-shock treatment. *Tg(hsp70l:noggin)*, *Tg(hsp70l:bmp2b)*, *Tg*(*hsp70l*:*vegfaa*$_{121}$;*cmlc2*:*GFP*) and *Tg(hsp70l:dnbmprI–GFP)* embryos were heat-shocked 25–26 hpf for 30 min at 42 °C. *Tg(hsp70l:noggin)* and *Tg(hsp70l:bmp2b)* embryos were genotyped by PCR, and *Tg*(*hsp70l*:*vegfaa*$_{121}$;*cmlc2*:*GFP*) and *Tg(hsp70l:dnbmprI–GFP)* embryos were identified by the expression of GFP.

Quantification. To quantify and compare arterial and venous angiogenesis in Figs 1b, 3b, 3h, 4b, 5b and Supplementary Figs S6a, S14a,b and S18b, we calculated the percentage of segments that form an angiogenic vessel from the dorsal aorta (ISA) or from the axial vein (CVP) between 36 and 40 hpf. Each segment is defined as the area on the anterior–posterior axis between two adjacent somite boundaries. The first 12 segments starting at the end of the yolk extension (roughly corresponding to the 14th to 26th somite) were analysed. To quantify arterial angiogenesis (red bars), each segment that contained an ISA (at the anterior somite boundary) that reached the dorsal longitudinal anastomotic vessel was given a value of 1, and each segment that lacked an ISA was given a value of 0. Similarly, to quantify venous angiogenesis (blue bars), each segment that contained a CVP with a fused ventral vein (therefore, completed the CV remodelling) was given a value of 1, and segments that lacked a fused ventral vein in the CVP were given a value of 0. These values were then used to calculate the percentage of segments with either ISA (red bars) or CVP (blue bars).

To quantify ectopic vessels in *bmp2b*-overexpressing embryos in Figs. 3d, 4d, 5b and Supplementary Figs S6b, S14b and S18c, embryos were examined between 44 and 50 hpf. As the ectopic sprouts and pairs of ISAs formed in both the left and right sides of the embryos, only the ISAs and sprouts closest to the objective were analysed.

To quantify embryos with somatic mosaicism in Fig. 3g,h, embryos were presorted for GFP expression in endothelial cells between 44 and 50 hpf. Only the mosaic segments (area between two adjacent somite boundaries) that contained patches of *kdrl:GFP*- or *kdrl:DNBmprI–GFP*-expressing endothelial cells were quantified. The number of endothelial branches per segment was counted, and an average was calculated (Fig. 3g). To calculate the percentage of mosaic segments that form a CVP (Fig. 3h), each segment that contained a CVP with a fused ventral vein was given a value of 1, and segments that lacked a fused ventral vein in the CVP were given a value of 0. These values were then used to calculate the percentage of segments with a CVP.

In all cases, embryos with gross morphological defects were presorted and excluded from analysis before quantification.

Morpholino injections and small-molecule treatment. Micro-injections of morpholino oligonucleotides were carried out as previously described[35]. Briefly, embryos were injected at the single-cell stage with 4–12 ng of control morpholino (Gene Tools), 12 ng of *bmpr2a* splicing morpholino #1, 12 ng of *bmpr2a* splicing morpholino #2, 8 ng of *bmpr2b* splicing morpholino #1, 12 ng of *bmpr2b* splicing morpholino #2 and a combination of 2 ng of *kdrl* and 2 ng of *kdr* morpholino (Gene Tools). Embryos were co-injected with 2 ng of p53 morpholino (Gene Tools) and embryos with gross morphological defects were presorted and excluded from quantification. The sequences for the morpholino oligonucleotides used in this study are: *bmpr2a* #1: 5′-AGAGAAACGTATTTGCATACCTTGC-3′; *bmpr2a* #2: 5′-TCATTACGGAAACATACCTCTTAGC-3′; *bmpr2b* #1: 5′-AGTTGATTCTGACCTTGTTTGACCA-3′; *bmpr2b* #2: 5′-CGGCTTCATCTTGTT-CTGACCTCAC-3′; *kdrl*: 5′-CACAAAAAGCGCACACTTACCATGT-3′ (ref. 5); and *kdr*: 5′-GTTTTCTTGATCTCACCTGAACCCT-3′ (ref. 5).

Embryos were treated with chemical inhibitors at 26 hpf. The final concentration of small-molecule inhibitors was 60 μM of SL327, 200 μM of SB203580, 40 μM of dorsomorphin, 10 μM of DMH1 and 5 μM of DMH1 in 2% DMSO.

Live-cell imaging and three-dimensional image processing. Embryos were dechorionated, and embedded in 1% agarose (containing egg water with tricaine) in the centre of a glass bottom Petri dish (MatTek). Once the agarose solidified, egg water with tricaine was added. Embryos were imaged using a Zeiss 510 Meta confocal microscope.

Zeiss LSM software was used to generate monochrome projections and three-dimensional (3D) colour projections from confocal *Z* stacks. The colour bar on the 3D colour projections represents the *z*-axis location of objects, with red representing the most proximal (closest to viewer) and blue representing the most distal blood vessels (farthest from viewer).

Real-time PCR. Quantitative real-time PCR for zebrafish *id2a*, *vegfa*, *vegfc*, *dll4* and *flt4* was carried out using the TaqMan gene expression assay (Applied Biosystems). Wild-type and *Tg*(*hsp70l*:*bmp2b*)$^{+/-}$ fish were incrossed and heat-shocked as previously described. Total RNA was extracted from ~50 embryos 2 h after heat-shock treatment and 5 h after heat-shock treatment. *Glyceraldehyde-3-phosphate dehydrogenase* (*gapdh*) was used as an endogenous control to normalize expression levels. The expression levels of *id2a*, *vegfa*, *vegfc*, *dll4* and *flt4* were displayed as a ratio of *bmp2b*-induced to wild-type expression level.

Generating transgenic constructs. The *vegfa* gene was amplified from complementary DNA of 32-hpf embryos. The PCR product was ligated into the pCR8 vector (Invitrogen). The *vegfa* gene was sequenced and found to be the *vegfaa*$_{121}$ splicing isoform. The gateway tol2 kit[36] was used to create the *hsp70l:vegfaa*$_{121}$ construct, which was injected with transposase RNA into one-cell embryos to create stable *Tg*(*hsp70l*:*vegfaa*$_{121}$;*cmlc2*:*EGFP*) transgenic lines.

The dominant-negative form of the Bmp receptor type I (*DNbmprI–GFP*) gene was amplified from the cDNA of *Tg(hsp70l:DNbmprI–GFP)* embryos[32], and ligated into the pCR8 vector (Invitrogen). The gateway tol2 kit was used to generate the *kdrl:DNbmprI–GFP* construct. The resulting construct was injected with transposase RNA into one-cell embryos, which generated patches of endothelial cells that overexpress the *DNbmprI–GFP* fusion protein.

27. Westerfield, M. *The Zebrafish Book, a Guide for the Laboratory Use of Zebrafish (Danio Rerio)* 4th edn (Univ. Oregon Press, 2000).
28. Roman, B. L. *et al.* Disruption of acvrl1 increases endothelial cell number in zebrafish cranial vessels. *Development* **129,** 3009–3019 (2002).
29. Jin, S. W., Beis, D., Mitchell, T., Chen, J. N. & Stainier, D. Y. Cellular and molecular analyses of vascular tube and lumen formation in zebrafish. *Development* **132,** 5199–5209 (2005).
30. Chi, N. C. *et al.* Genetic and physiologic dissection of the vertebrate cardiac conduction system. *PLoS Biol.* **6,** 1006–1019 (2008).
31. Chocron, S., Verhoeven, M. C., Rentzsch, F., Hammerschmidt, M. & Bakkers, J. Zebrafish Bmp4 regulates left-right asymmetry at two distinct developmental time points. *Dev. Biol.* **305,** 577–588 (2007).
32. Pyati, U. J., Webb, A. E. & Kimelman, D. Transgenic zebrafish reveal stage-specific roles for Bmp signalling in ventral and posterior mesoderm development. *Development* **132,** 2333–2343 (2005).
33. Thisse, B. *et al.* Expression of the zebrafish genome during embryogenesis. ZFIN Direct Data Submission (http://zfin.org/cgi-bin/webdriver?MIval=aa-pubview2.apg&OID=ZDB-PUB-010810-1) (2001).
34. Thisse, C. & Thisse, B. *Zebrafish Science Monitor, Vol. 5.* (Univ. Oregon Press, 1998).
35. Nasevicius, A. & Ekker, S. C. Effective targeted gene 'knockdown' in zebrafish. *Nat. Genet.* **26,** 216–220 (2000).
36. Kwan, *et al.* The Tol2kit: a multisite gateway-based construction kit for Tol2 transposon transgenesis constructs. *Dev. Dyn.* **236,** 3088–3099 (2007).

nature cell biology

DOI: 10.1038/ncb2232

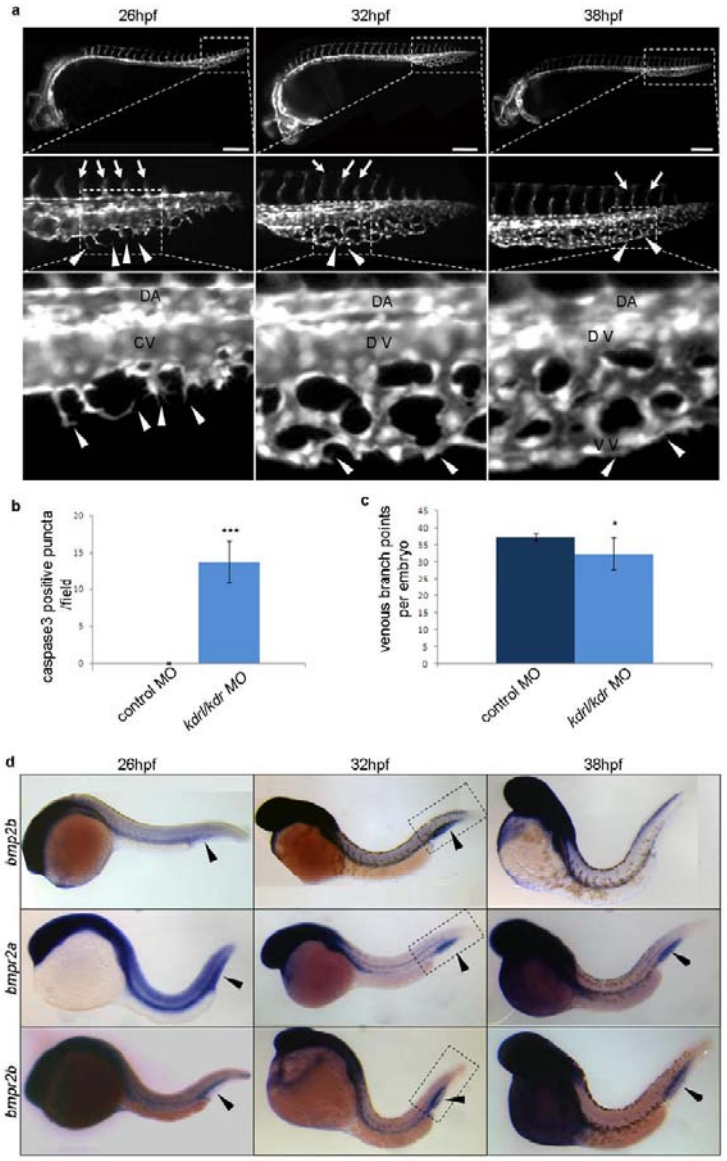

Figure S1 Vegf-A signal is dispensable for the formation of Caudal Vein Plexus (CVP), and endothelial cells within the angiogenic region of the axial vein (AV) express Bmp pathway components. (**a**) Epiflourescent micrographs of *Tg(kdrl:GFP)* embryos at 26hpf, 32hpf, and 38hpf. Areas within dashed rectangles are shown with higher resolution in the panel below. Endothelial cell sprouts from the dorsal aorta form the ISAs (arrows). Angiogenic extensions sprout from the AV at 26hpf and establish connections with neighboring sprouts by 32hpf (arrowheads). These endothelial cell connections are stabilized leading to the formation of a mature AV plexus by 38hpf (arrowheads). The AV plexus is a fenestrated network composed of a dorsal (DV) and ventral vein (VV) with interconnecting vessels. Scale bar, 250μm. Abbreviations: DA, dorsal aorta; VV, ventral vein; DV, axial vein. (**b**) *Tg(kdrl:GFP)* embryos were injected with either control or *kdrl/b* MOs and stained for cleaved-Caspase3 at 34hpf. A 40x objective was used to analyze endothelial cells in the tail. The number of cleaved-caspase3 positive endothelial cell puncta per field of view was counted and quantified in control (n=5) and *kdrl/b* (n=4) MO injected embryos. No cleaved-Caspase3 positive puncta in endothelial cells were observed in the control injected embryos, while *kdrl/b* morphant embryos contained on average 13.75 cleaved-Caspase3 positive endothelial cells per field. Error bars represent mean ± SEM. ***P<0.001 versus control, Student's *t* test. (**c**) *Tg(kdrl:GFP)* embryos were injected with either control or *kdrl/b* MOs and the number of venous branch points were counted in control (n=5) and *kdrl/b* (n=7) MO injected embryos. The number of venous branch points in *kdrl/b* MO injected embryos was marginally decreased compared to control MO injected embryos (37.2 in control vs 32.4 in *kdrl/kdrb* MO injected embryos). Error bars represent mean ± SEM. *P<0.05 versus control, Student's *t* test. (**d**) Micrographs are of embryos at 26hpf, 32hpf, and 38hpf after *in situ* hybridization with *bmp2b*, *bmpr2a*, or *bmpr2b*. Bmp signaling components show high reactivity within the developing CV plexus (black arrow heads). Dashed boxes indicate the areas magnified in Fig. 1.

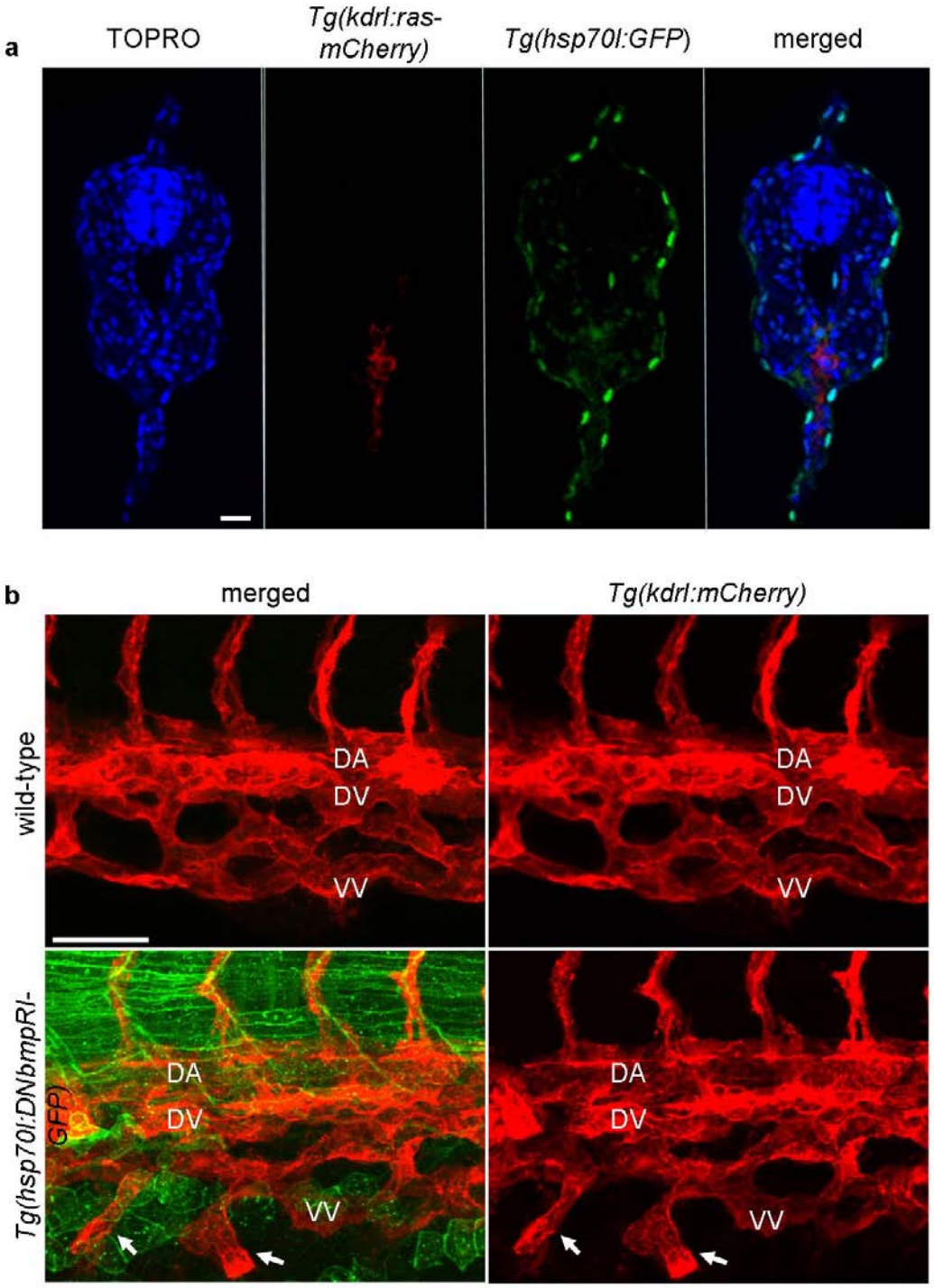

Figure S2 Activation of the *hsp70l* promoter drives quasi-ubiquitous expression of GFP in *Tg(hsp70l:GFP)* embryos, and effectively blocks CVP formation in *Tg(hsp70l:DNbmprI-GFP)* embryos. (**a**) *Tg(hsp70l:GFP)* embryos were heat-shocked and sectioned at 42hpf. Merged image indicates that GFP is expressed in the majority of non-neural cells. (**b**) Wild-type and *Tg(hsp70l:DNbmprI-GFP)* embryos were heat-shocked at 23hpf for 30minutes at 42°C. Wild-type embryos do not express DNbmprI-GFP and have a properly formed CVP. *Tg(hsp70l:DNbmprI-GFP)* embryos express DNbmprI-GFP following heat-shock and have CVP defects (arrows). Scale bar, 50μm. Abbreviations: DA, dorsal aorta; VV, ventral vein; DV, dorsal vein.

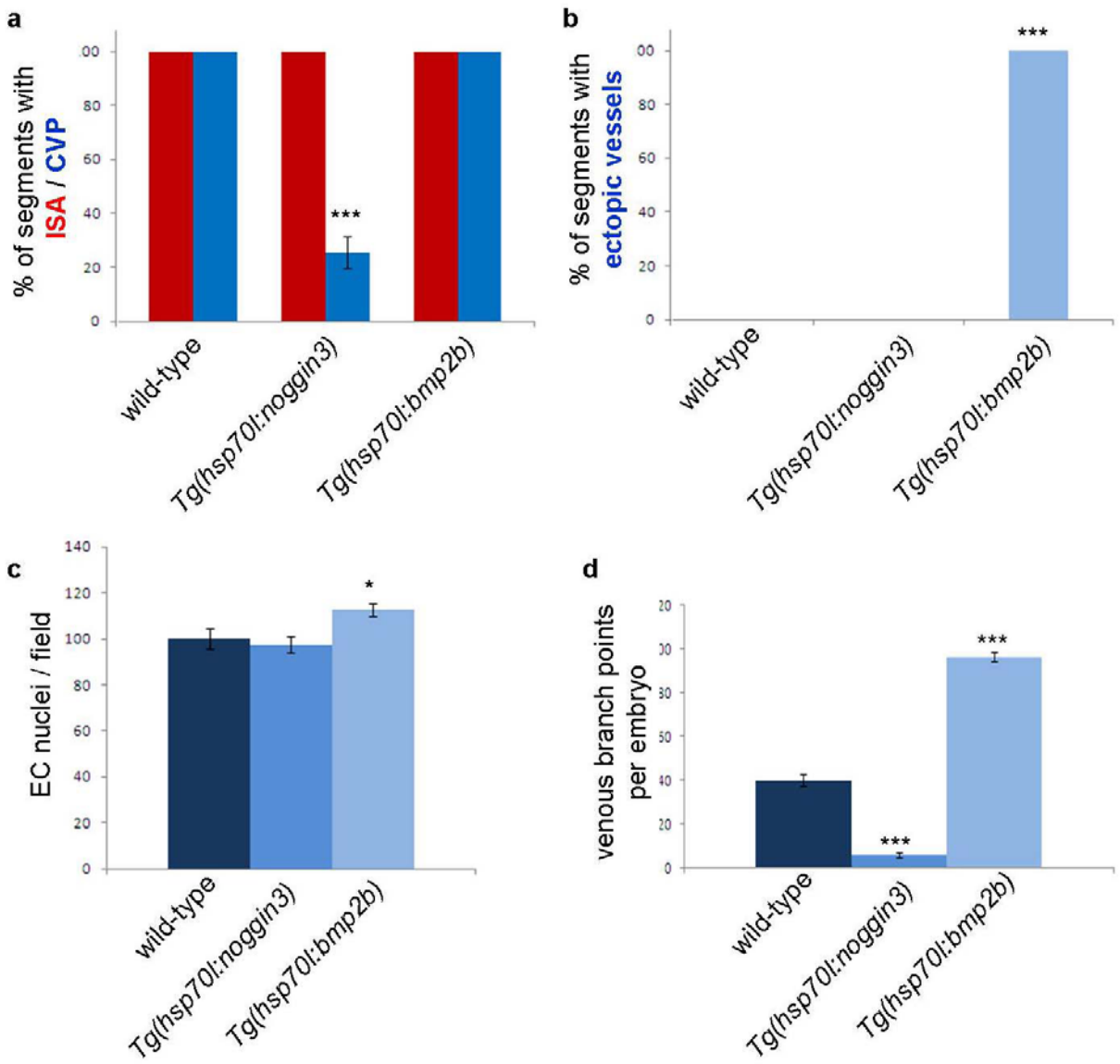

Figure S3 Bmp signaling regulates CVP formation by affecting endothelial cell number and venous branching. (**a**) The percentage of segments that contain an ISA (red bars) or a CVP (blue bars) was quantified in wild-type (n=6), *Tg(hsp70l:noggin3)* (n=6), and *Tg(hsp70l:bmp2b)* (n=6) embryos. Over-expression of *noggin3* blocked the formation of CVP but not ISAs. (**b**) The percentage of segments containing ectopic vessels was quantified in wild-type (n=6), *Tg(hsp70l:noggin3)* (n=6), and *Tg(hsp70l:bmp2b)* (n=6). *bmp2b* over-expression causes robust ectopic vessel formation. Error bars represent mean ± SEM. ***P<0.001 versus control, Student's *t* test. (**c**) The number of endothelial cells in the CVP of *Tg(fli1:nEGFP)* embryos with wild-type (n=6), *Tg(hsp70l:noggin3)* (n=6), *Tg(hsp70l:bmp2b)* (n=6) background was quantified. The number of endothelial cell nuclei per field of view is displayed. The average number of endothelial cells in *noggin3* over-expressing embryos was not significantly decreased, but the average number of endothelial cells in *bmp2b* over-expressing embryos was increased by 12.5%. (**d**) Branch point analysis of CVP demonstrated that *noggin3* over-expressing embryos exhibited decreased branching, while *bmp2b* over-expressing embryos exhibited increased branching (n=3 for wild-type, n=4 for *Tg(hsp70l:noggin3)*, and n=4 for *Tg(hsp70l:bmp2b)*). Error bars represent mean ± SEM. *P<0.05 and ***P<0.001 versus control, Student's *t* test.

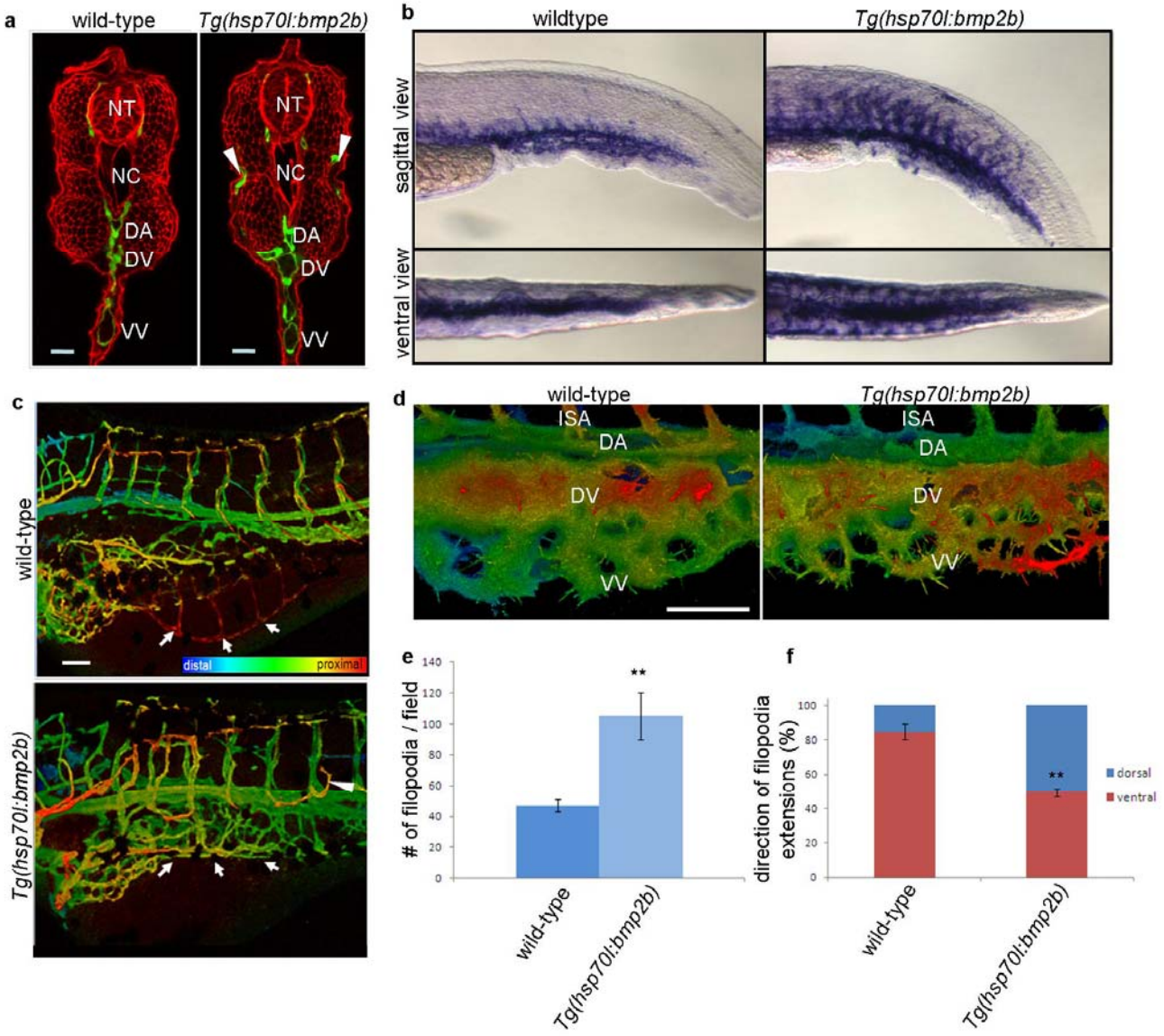

Figure S4 Bmp signaling promotes angiogenesis from the CVP. (**a**) Wild-type and *Tg(hsp70:bmp2b)* embryos were sectioned in the transverse plane at 48hpf and stained for β-tubulin (red) to outline cells. Ectopic vessels in *Tg(hsp70:bmp2b)* embryos formed between the epithelial surface and the somite boundary (arrows). Scale bars, 20μm. Abbreviations: DA, dorsal aorta;VV, ventral vein; DV, dorsal vein; NC, notocord; NT, neural tube. (**b**) Wild-type and *Tg(hsp70:bmp2b)* embryos were heat-shocked and subsequently fixed at 30 hpf. A marker of venous endothelium, *dab2*, was strongly expressed in the ectopic vessels that emanated from the AV in *Tg(hsp70:bmp2b)* embryos. (**c**) Representative images of the subintestinal vein plexuses (SIVP) of 84hpf *Tg(kdrl:GFP)* and *Tg(hsp70l:bmp2b); Tg(kdrl:GFP)* embryos that were heat-shocked at 60hpf. Confocal Z-stacks were converted into heat-map projections and scale bars represent the proximity of vessels. The SIVP in *Tg(kdrl:GFP)* embryos contains stereotypical ventral projections (arrows); *bmp2* over-expression shifted SIVP vessels dorsally (arrows) and induced ectopic sprouts (arrowheads). Scale bar, 50μm. (**d**) Wild-type and *Tg(hsp70l:bmp2b)* embryos were analyzed 4 hr post heat-shock. Filopodia were imaged in the *Tg(kdrl:ras-mCherry)* transgenic background, and Z-stacks were assembled in a heat map as described in previous legends. (**e**) The number of filopodia was quantified. *bmp2b* over-expressing embryos contained more filopodia per field compared to control. (**f**) The angle of the filopodia projections relative to the dorsal aorta was analyzed. While the majority of wild-type filopodia extended in the ventral direction (84.8 percent), filopodia angle in *bmp2b* over-expressing embryos was randomized. wild-type, n=4; *Tg(hsp70l:bmp2b)* n=4 embryos. Error bars represent mean ± SEM. **P<0.01 versus control, Student's *t* test. Abbreviations: DA, dorsal aorta; ISA, intersegmental artery; VV, ventral vein; DV, dorsal vein.

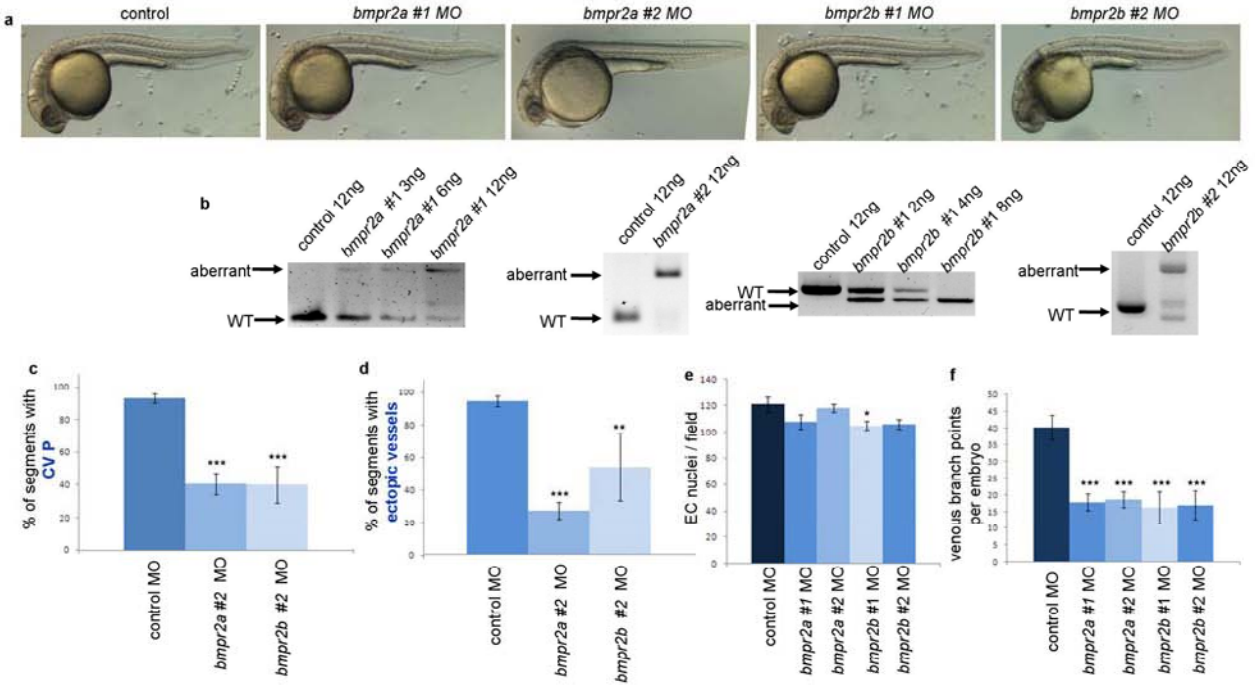

Figure S5 Both *bmpr2a* **and** *bmpr2b* are necessary for venous angiogenesis. (**a**) Brightfield images of 32hpf embryos injected with control, *bmpr2a #1*, *bmpr2a #2, bmpr2b* #1, or *bmpr2b* #2 MO. (**b**) PCR analyses from morphant cDNA demonstrate the efficiency of each splicing MO. (**c**) WT embryos or (**d**) *Tg(hsp70l:bmp2b)* embryos were injected with *bmpr2a* #2 and *bmpr2b* #2 splicing MOs. (**c**) The percentage of segments that contain a CVP was quantified in control (n=48), *bmpr2a* #2 (n=40), and *bmpr2b* #2 (n=20) MO injected embryos. (**d**) The percentage of segments that contain an ectopic vessel was quantified in control (n=32), *bmpr2a* #2 (n=38), and *bmpr2b* #2 MO (n=15) injected embryos. *bmpr2a* #2 and *bmpr2b* #2 splicing MOs inhibited the formation of the CVP and ectopic vessels. Error bars represent mean ± SEM. **P<0.01 and ***P<0.001 versus control, Student's *t* test. (**e**) The number of endothelial cells in the CVP region of *Tg(fli1:nEGFP)* embryos was quantified by counting the number of endothelial cell nuclei per field of view in control (n=7), *bmpr2a* #1(n=7), *bmpr2a* #2 (n=7); *bmpr2b* #1 (n=7), and *bmpr2b* #2 (n=7) MO injected embryos. (**f**) Branch point analysis of venous networks was performed in control (n=11), *bmpr2a* #1 (n=13), *bmpr2a* #2 (n=24), *bmpr2b* #1 (n=10), and *bmpr2b* #2 (n=12) MO injected embryos. *bmpr2a* and *bmpr2b* morphants exhibited significantly decreased branching. Error bars represent mean ± SEM. *P<0.05 and ***P<0.001 versus control, Student's *t* test.

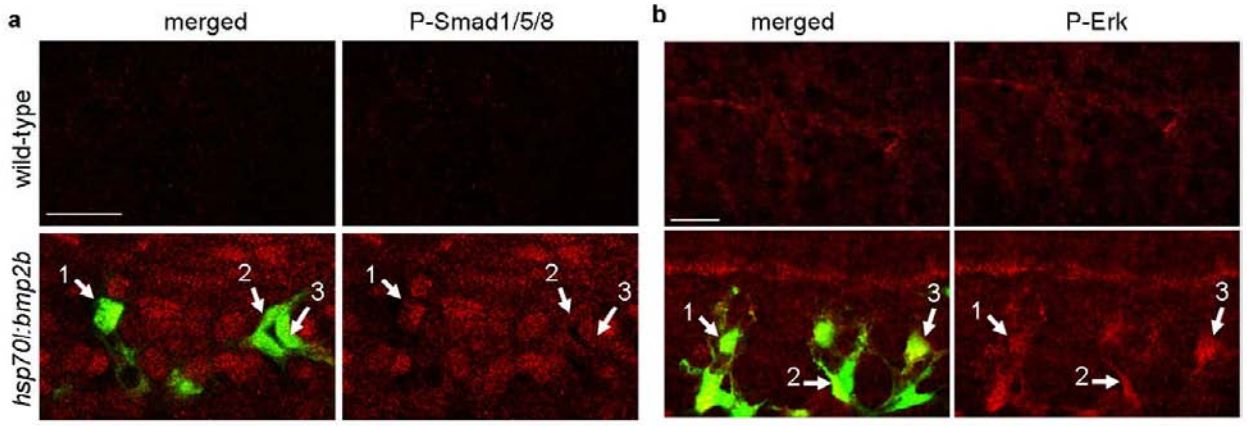

Figure S6 P-Smad and P-Erk are expressed in Bmp-induced sprouts. *Tg(kdrl:GFP)* wild-type and *Tg(hsp70l:bmp2b);Tg(kdrl:GFP)* heat-shocked embryos were stained with (a) phospho-Smad1/5/8 or (b) phospho-Erk. Confocal images were taken between the epithelial surface and the somite boundary, where Bmp-induced ectopic sprouts form. Numbered arrows indicate Bmp-induced ectopic endothelial cells that express either phospho-Smad1/5/8 or phospho-Erk

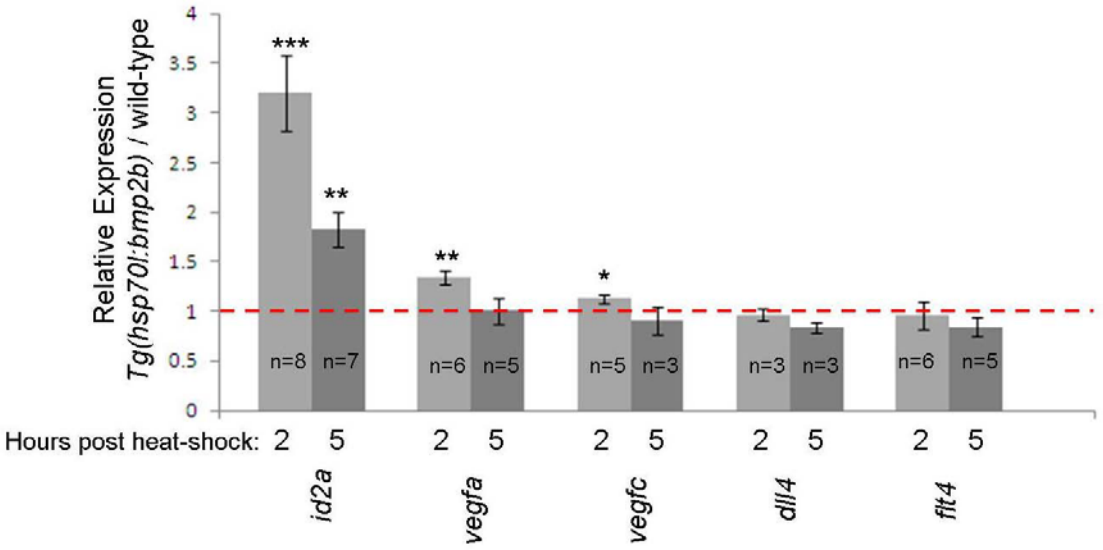

Figure S7 The effects of *bmp2b* over-expression on transcription levels of selected genes. Gene expression level of *bmp2b* over-expressing embryos was compared to wild-type embryos using quantitative RT-PCR. At 2 hr post heat-shock (light gray bars), transcription of a known Bmp target gene, *id2a*, was increased by 3.2 fold (P<0.001), while those of *vegfa* and *vegfc* were moderately increased (P=0.0042 and P=0.483 respectively), and transcription of *dll4* and *flt4* was unaffected. At 5 hr post heat-shock (dark gray bars) *id2a* was the only transcript increased (P=0.0029). n = the number of independent RNA samples/experiments (Error bars represent mean ± SEM. *P<0.05, **P<0.01, **P<0.001, one sample *t* test.)

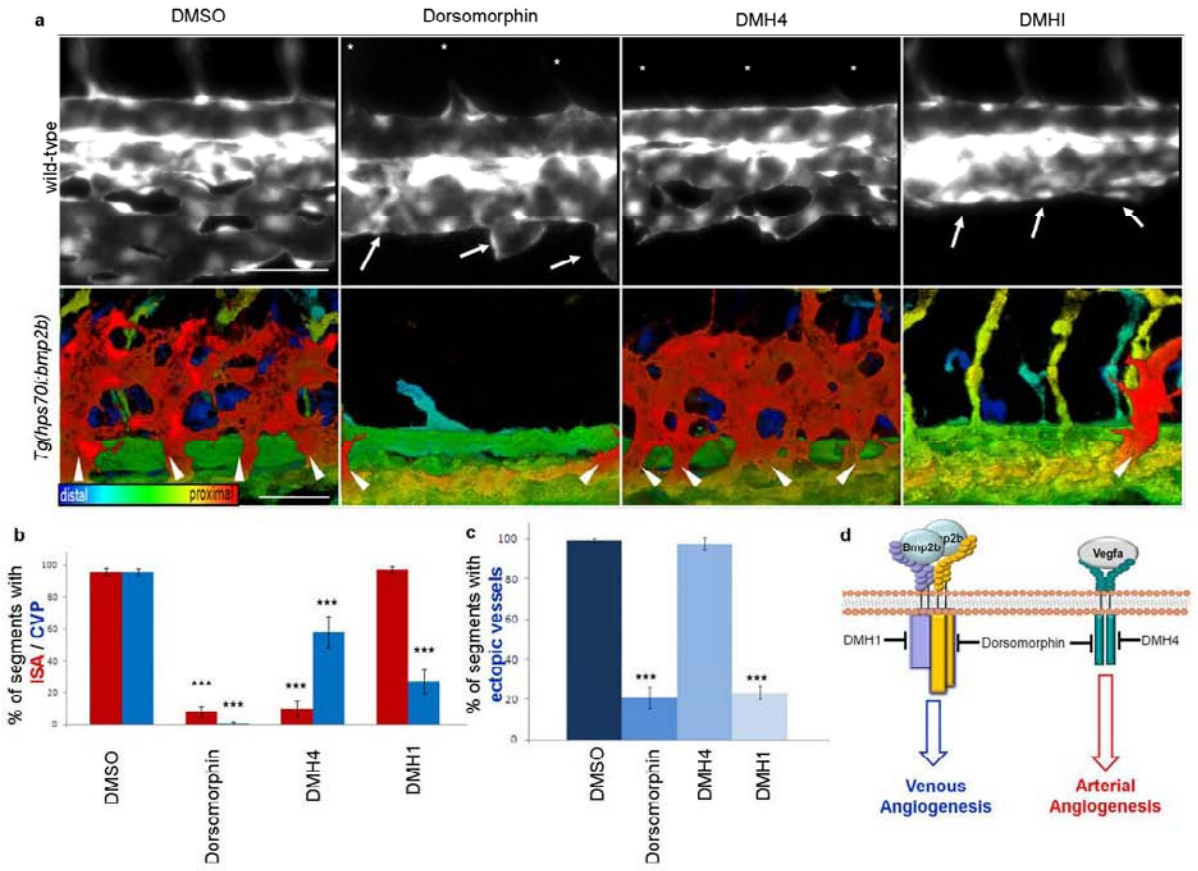

Figure S8 Distinct functions of Bmp and Vegf-A signaling during angiogenesis. (a) Epiflourescent micrographs of 38hpf *Tg(kdrl:GFP)* embryos (top panel) and *Tg(hsp70l:bmp2b); Tg(kdrl:GFP)* embryos (bottom panel) treated with DMSO, dorsomorphin (blocking both Vegf-A and Bmp signaling), DMH4 (blocking Vegf-A signaling), and DMH1 (blocking Bmp signaling). Arrows in the top panel point defective formation of venous sprouts ventrally, asterisks point defective formation of arterial sprouts dorsally, and arrowheads in the bottom panel point to ectopic venous sprouts. (b) The percentage of segments that contain an ISA (red bars) or a CVP (blue bars) was quantified in DMSO (n=14), dorsomorphin (n=13), DMH4 (n=6), and DMH1 (n=13) treated embryos. In dorsomorphin-treated embryos, formation of both ISA and CVP was significantly reduced. Treatment with DMH4, a specific inhibitor of Vegf-A signaling, preferentially blocks formation of ISA. Addition of DMH1, a specific inhibitor of Bmp signaling, selectively blocks formation of CVP. (c) The percentage of segments that contain ectopic vessels (green bars) was quantified in DMSO (n=11), dorsomorphin (n=6), DMH4 (n=5), DMH1 (n=13) treated embryos. The formation of Bmp-induced venous sprouts is inhibited by dorsomorphin or DMH1 treatment, but not by DMH4 treatment. (d) Schematic diagram showing the specific targets of each small chemical inhibitor used in this study. Error bars represent mean ± SEM. ***P<0.001 versus control, Student's *t* test.

Supplemental Movie Legends

MovieS1 Time lapse imaging of wild-type embryos. Developing CV plexus region of 32hpf *Tg(fli1:nGFP);Tg(kdrl:ras-mCherry)* embryos was imaged for 3 hours.

MovieS2 Time lapse imaging of *noggin3* over-expressing embryos. Developing CV plexus region of 32hpf *Tg(fli1:nGFP);Tg(kdrl:ras-mCherry)* embryos was imaged for 3 hours.

MovieS3 Time lapse imaging of *bmp2b* over-expressing embryos. Developing CV plexus region of 32hpf *Tg(fli1:nGFP);Tg(kdrl:ras-mCherry)* embryos was imaged for 3 hours.

MovieS4 Time lapse imaging of GFP expressing endothelial cells. The *kdrl:GFP* construct was mosaically expressed in *Tg(kdrl:ras-mCherry)* embryos. The CV plexus was imaged starting at 29hpf for 5.5hrs.

MovieS5 Time lapse imaging of DNBmprI-GFP expressing endothelial cells. The *kdrl:DNBmpr1-GFP* construct was mosaically expressed in *Tg(kdrl:ras-mCherry)* embryos. The CV plexus was imaged starting at 29hpf for 5.5hrs.